

## Research Article

# Interplay between negative and positive design elements in $G\alpha$ helical domains of G proteins determines interaction specificity toward RGS2

Mohammad Kasom, Samia Gharra, Isra Sadiya, Meirav Avital-Shacham and  Mickey Kosloff

Department of Human Biology, Faculty of Natural Science, University of Haifa, Haifa 3498838, Israel

**Correspondence:** Mickey Kosloff (kosloff@sci.haifa.ac.il)

Regulators of G protein signaling (RGS) proteins inactivate  $G\alpha$  subunits, thereby controlling G protein-coupled signaling networks. Among all RGS proteins, RGS2 is unique in interacting only with the  $G\alpha_q$  but not with the  $G\alpha_i$  subfamily. Previous studies suggested that this specificity is determined by the RGS domain and, in particular, by three RGS2-specific residues that lead to a unique mode of interaction with  $G\alpha_q$ . This interaction was further proposed to act through contacts with the  $G\alpha$  GTPase domain. Here, we combined energy calculations and GTPase activity measurements to determine which  $G\alpha$  residues dictate specificity toward RGS2. We identified putative specificity-determining residues in the  $G\alpha$  helical domain, which among G proteins is found only in  $G\alpha$  subunits. Replacing these helical domain residues in  $G\alpha_i$  with their  $G\alpha_q$  counterparts resulted in a dramatic specificity switch toward RGS2. We further show that  $G\alpha$ -RGS2 specificity is set by  $G\alpha_i$  residues that perturb interactions with RGS2, and by  $G\alpha_q$  residues that enhance these interactions. These results show, for the first time, that the  $G\alpha$  helical domain is central to dictating specificity toward RGS2, suggesting that this domain plays a general role in governing  $G\alpha$ -RGS specificity. Our insights provide new options for manipulating RGS-G protein interactions *in vivo*, for better understanding of their ‘wiring’ into signaling networks, and for devising novel drugs targeting such interactions.

## Introduction

Heterotrimeric ( $\alpha\beta\gamma$ ) G proteins are molecular switches that mediate signaling initiated by G protein-coupled receptors (GPCRs) and play central roles in numerous cellular signaling cascades [1–3]. G proteins are activated by the exchange of bound GDP nucleotide within the  $G\alpha$  subunit for GTP, enabling the  $G\alpha$  subunit to stimulate downstream effectors. The activity of  $G\alpha$  subunits is terminated by interaction with regulators of G protein signaling (RGS) proteins. The RGS domain in these proteins accelerates GTP hydrolysis by the  $G\alpha$  subunit, thereby acting as a GTPase-activating protein (GAP) [4–8]. Based on their sequence similarities,  $G\alpha$  subunits are divided into the  $G_s$ ,  $G_i$ ,  $G_q$ , and  $G_{12/13}$  subfamilies. The 20 ‘canonical’ RGS proteins, which are organized into four subfamilies (R4, R7, R12, and RZ), can potentially recognize and inactivate  $G\alpha$  subunits from the  $G_i$  and  $G_q$  subfamilies [9]. However, the molecular determinants of  $G\alpha$ -RGS specificity remain to be fully defined [10].

In all  $G\alpha$ -RGS complex structures that were solved experimentally to date, the RGS domain binds to the GTPase domain of the  $G\alpha$  subunit [11–17]. Previous structural and biochemical studies have further shown that three substructures within the GTPase domain (termed switches I, II, and III) play central roles in mediating interactions with RGS domains [2,10,11,14–20]. On the other hand, the  $G\alpha$  subunit contains a second domain, the  $G\alpha$  helical domain, which can also interact with RGS domains [10,13,14,16,17]. For years, the biological role of the  $G\alpha$  helical domain, which among all G proteins is unique to  $G\alpha$  subunits, was unclear [21], although it was previously implicated in increasing affinity for GTP [22], acting as a tethered intrinsic GAP [23], or participating in effector recognition [24].

Received: 11 April 2018  
Revised: 18 June 2018  
Accepted: 19 June 2018

Accepted Manuscript online:  
20 June 2018  
Version of Record published:  
25 July 2018

More recently, it was shown that the  $G\alpha$  helical domain mediates binding to inhibitory proteins, such as guanine-nucleotide dissociation inhibitors [25], and plays a central role in  $G\alpha$  activation by GPCRs and nucleotide exchange [26]. Previous structural studies observed that RGS contacts with the  $G\alpha$  helical domain can be heterogenic, suggesting that they might contribute to interaction specificity [13–17]. However, previous studies did not show a functional role for the  $G\alpha$  helical domain in interactions with RGS proteins, and particularly, in determining the specificity of these interactions.

Among the 20 canonical RGS proteins, RGS2 is unique in its extreme specificity for members of the  $G_q$  subfamily, showing no measurable GAP activity or affinity toward any member of the  $G_i$  subfamily [27]. RGS2 is involved in many physiological functions, such as blood pressure homeostasis [28,29], cardiac function [30–33], airway contraction [34,35], immunity [36], and synaptic function [36–39]. RGS2 was shown to play crucial roles in mental disorders, such as anxiety, depression, and stress [36,40–42], and has been implicated in numerous pathological conditions, such as hypertension [43–46], cardiac hypertrophy [47], bacterial infection [48], and various cancers [49–54]. Presumably, these varied biological roles are dependent on the interaction specificity of RGS2. To identify the basis for RGS2 selectivity, Heximer et al. [55] compared the sequences of RGS2 and other RGS proteins and identified three crucial residues that are highly conserved among the RGS family, yet differ in RGS2. These RGS2 residues (C106, N184, and E191) are located at the interface with the  $G\alpha$  subunit and were suggested to prevent RGS2 activity toward the  $G_i$  subfamily [15,55]. Exchanging these three residues for their RGS4 counterparts yielded a gain-of-function phenotype that enabled the triple-mutant RGS2 to bind and down-regulate  $G\alpha_i$  [15,55]. More recently, the structure of the  $G\alpha_q$ -RGS2 complex showed that RGS2 adopts a unique pose believed to enable interaction with the  $G\alpha_q$  switch regions [16]. A subsequent structure of  $G\alpha_q$ -RGS8 [17] and comparison with previous  $G\alpha_i$ -RGS structures [11,14,15] revealed the manner with which RGS2 complexed with  $G\alpha_q$  was indeed unique; all other RGS domains bind their  $G\alpha$  partners similarly. Taken together, these studies concluded that the unique sequence of RGS2 leads to a distinct mode of interaction with  $G\alpha_q$  which, via interactions with the  $G\alpha$  switch regions in the GTPase domain, determines RGS2 specificity and its inability to inactivate members of the  $G_i$  subfamily [14–17]. Yet, it was not shown experimentally whether interaction specificity with RGS2 is indeed determined by the GTPase domain of  $G\alpha$  subunits.

We have previously shown that several  $G\alpha_i$  helical domain residues substantially contribute to interactions with RGS domains [10]. Here, we extended our energy calculations to compare RGS complexes with  $G\alpha_i$  and  $G\alpha_q$ . Our analysis identified helical domain residues that can dictate specificity toward RGS proteins in general and toward RGS2 in particular. Analyzing these residues at the 3D structure level allowed us to predict  $G\alpha_i$  residues that would perturb interactions with RGS2, as well as  $G\alpha_q$  residues that would favorably contribute to such interactions. These computational predictions were validated by  $G\alpha_i$ -to- $G\alpha_q$  mutagenesis, showing that substitutions in the  $G\alpha$  helical domain were sufficient for an RGS2 specificity switch toward  $G\alpha_i$ .

## Materials and methods

### Protein structures and sequences

We used the following 3D structures in our analysis and visualization of  $G\alpha$ -RGS complexes (with PDB codes for each structure):  $G\alpha_{i1}$ -RGS4 (1AGR) [11],  $G\alpha_{i1}$ -RGS16 (2IK8) [14],  $G\alpha_{i1}$ -RGS1 (2GTP) [14],  $G\alpha_q$ -RGS2 (4EKD) [16], and  $G\alpha_q$ -RGS8 (5DO9) [17]. Missing short segments in PDB entry 2IK8 ( $G\alpha_{i1}$  residues 112–118) were modeled on the basis of the  $G\alpha_{i1}$ -RGS4 structure (PDB 1AGR) using the program Nest [56], with partial or missing side chains being modeled using Scap [57]. 3D structural visualization and superimposition were carried out with PyMol (<http://pymol.org>).

### Energy calculations for identifying $G\alpha_{i/q}$ residues determining specificity toward RGS2

We followed the methodology described previously [10,58,59] to analyze the per-residue contributions of  $G\alpha$  residues to their RGS partners in the crystal structures mentioned above. We used the finite difference Poisson–Boltzmann (FDPB) method to calculate the net electrostatic and polar contributions ( $\Delta\Delta G_{\text{elec}}$ ) of each residue within 15 Å of the dimer interface. Residues that substantially contribute to the interaction were defined as those contributing  $\Delta\Delta G_{\text{elec}} \geq 1$  kcal/mol to the interactions (i.e. twice the numerical error of the electrostatic calculations) [60]. Non-polar energy contributions ( $\Delta\Delta G_{\text{np}}$ ) were calculated as a surface–area proportional term, by multiplying the per-residue surface area buried upon complex formation using surfv [61] by a

surface tension constant of  $-0.05 \text{ kcal/mol/\AA}^2$  [60]. Residues that substantially contribute to binding were defined as those contributing  $\Delta\Delta G_{\text{np}} \geq 0.5 \text{ kcal/mol}$  to the interactions (namely, bury more than  $10 \text{ \AA}^2$  of each protein surface upon complex formation).

## Protein expression, purification, and mutagenesis

The human RGS2 domain (residues 70–211) [15,55] and  $G\alpha_{i1}$  (residues 31–354) [25] were expressed using the pNIC-SGC1 (Addgene) and pProEXHTb (Invitrogen) vectors, respectively.  $G\alpha_{i1}$  mutants were produced using a QuikChange site-directed mutagenesis kit (Invitrogen). Proteins were expressed in *Escherichia coli* BL21 (DE3) cells and grown in 0.5 or 1 l of LB broth at  $37^\circ\text{C}$  for RGS or  $G\alpha$  protein expression, respectively, until an  $A_{600 \text{ nm}} \geq 1.4$  was reached. The temperature was then reduced to  $15^\circ\text{C}$  and protein expression was induced by the addition of 500 or 100  $\mu\text{M}$  isopropyl-D-thiogalactopyranoside for RGS or  $G\alpha$  proteins, respectively. After 16–18 h, cells were harvested by centrifugation at 6000 g for 30 min at  $4^\circ\text{C}$ , followed by freezing the pellets at  $-80^\circ\text{C}$ . Bacterial pellets were suspended in lysis buffer [50 mM Tris-HCl (pH 8.0), 50 mM NaCl, 5 mM  $\text{MgCl}_2$ , 5 mM  $\beta$ -mercaptoethanol, protease inhibitor cocktail (Roche), and 0.5 mM PMSF (for G proteins only)], and the cells were lysed using a Sonic Vibra-Cell sonicator, followed by centrifugation at 24 000 g for 30 min at  $4^\circ\text{C}$ . The supernatants were equilibrated to 500 mM NaCl and 20 mM imidazole and loaded onto 1 ml HisTrapFF columns (GE Healthcare Life Sciences). The columns were washed with >20 volumes of wash buffer [20 mM Tris-HCl (pH 8.0), 500 mM NaCl, and 20 mM imidazole] at  $4^\circ\text{C}$  and the tagged proteins were eluted with elution buffer [20 mM Tris-HCl (pH 8.0), 500 mM NaCl, and 100 mM imidazole]. The elute was loaded onto a HiLoad 16/600 Superdex 75 PG gel filtration column (GE Healthcare Life Sciences) at  $4^\circ\text{C}$  with  $\geq 1.5$  volumes of GF elution buffer [50 mM Tris-HCl (pH 8.0), 50 mM NaCl, 5 mM  $\beta$ -mercaptoethanol, and 1 mM  $\text{MgCl}_2$  (for  $G\alpha$  subunits only)]. The elute was dialyzed against dialysis buffer [GF elution buffer containing 40% glycerol (v/v)]. All purified proteins were estimated to be >95% pure, as assessed by SDS-PAGE electrophoresis and Coomassie staining. Protein concentrations were determined by measuring absorption at  $A_{280 \text{ nm}}$ , using predicted extinction coefficients (ProtParam, Swiss Institute for Bioinformatics) based on the sequence of each expressed protein.

## RGS GAP activity dose–response analysis

RGS activity measurements using dose–response analysis were performed as in previous studies [16,62]. Wild-type and mutant  $G\alpha_{i1}$  proteins were loaded with 1  $\mu\text{M}$  [ $\gamma$ - $^{32}\text{P}$ ]-GTP for 15 min at  $30^\circ\text{C}$  in reaction buffer [50 mM HEPES (pH 7.5), 0.05% polyoxyethylene (v/v), 5 mM EDTA, 5  $\mu\text{g/ml}$  BSA, and 1 mM dithiothreitol] and then cooled on ice for 5 min. Each assay was initiated by adding RGS protein at different concentrations in assay buffer (5 mM  $\text{MgCl}_2$  and 100  $\mu\text{M}$  cold GTP) to a tube containing  $G\alpha_{i1}$  (500 nM) on ice. Each reaction was terminated after 30 s by adding 100  $\mu\text{l}$  of 5% perchloric acid and quenched with 700  $\mu\text{l}$  of 10% (w/v) charcoal slurry in 50 mM phosphate buffer (pH 7.5), followed by centrifugation at 12 000 g for 5 min at room temperature. Aliquots (200  $\mu\text{l}$ ) of the supernatants were transferred to 3 ml scintillation fluid and analyzed using a Tri-Carb 2810 TR scintillation counter (PerkinElmer).  $\text{EC}_{50}$  values were determined from a three-parameter sigmoidal curve using SigmaPlot 10.0.

## Results

### $G\alpha_{i/q}$ residues that determine specificity toward RGS2 are located in the $G\alpha$ helical domain

To identify  $G\alpha$  residues that underlie specific RGS recognition by the  $G_i$  and  $G_q$  subfamilies, we applied energy-based calculations to compare which  $G\alpha_{i1}$  and  $G\alpha_q$  residues substantially contribute to interactions with RGS proteins in the relevant X-ray structures of  $G\alpha$ -RGS complexes. Using the computational methodology we developed [10,58,59], the three available X-ray structures of  $G\alpha_{i1}$  bound to the high-activity RGS domains RGS1, 4, 16 [11,14] were compared with the two available structures of  $G\alpha_q$  bound to RGS2 and RGS8 [16,17]. We used the FDPB method to calculate the net electrostatic and polar contributions ( $\Delta\Delta G_{\text{elec}}$ ) of each  $G\alpha$  residue that is within  $15 \text{ \AA}$  of the  $G\alpha$ -RGS interface in each complex. Non-polar energy contributions ( $\Delta\Delta G_{\text{np}}$ ) were calculated as a surface–area proportional term by multiplying the per-residue surface area buried upon complex formation by a surface tension constant of  $-0.05 \text{ kcal/mol/\AA}^2$ .

Our calculations showed that the majority of  $G\alpha_{i1}$  and  $G\alpha_q$  residues contributing to interactions with RGS domains do so electrostatically (Figure 1A–E; Supplementary Figures S1 and S2). About two-thirds of the

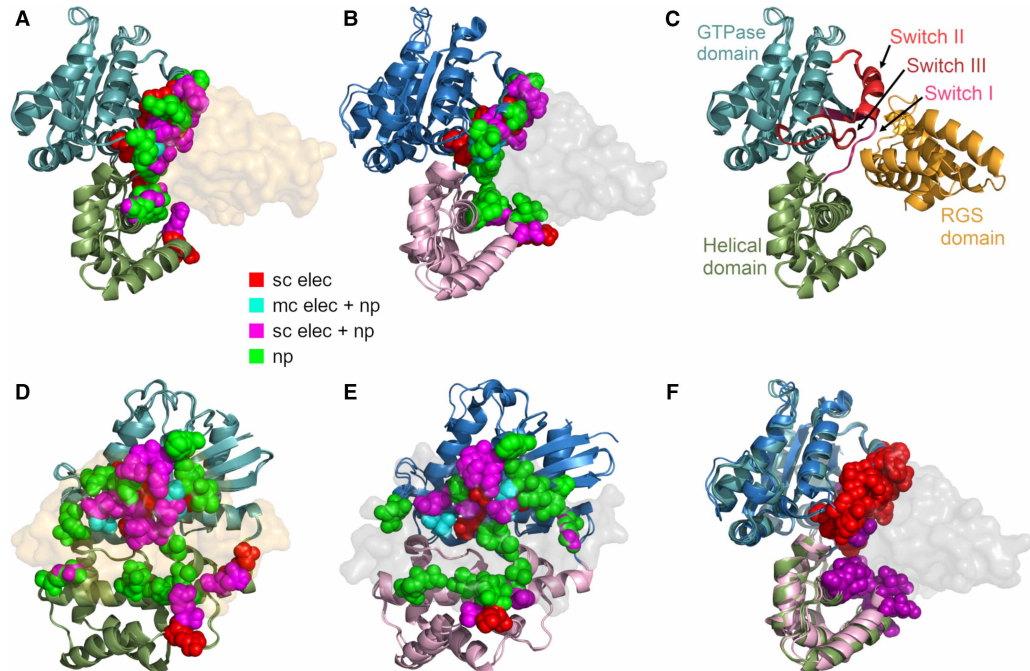


**Figure 1.  $G\alpha$  S&C residues are restricted to the GTPase domain, while putative  $G_{i/q}$  specificity-determining residues are mainly located in the helical domain.**

(A)  $G\alpha_{i1}$  residues that substantially contribute to interactions with high-activity RGS proteins, shown as spheres and colored according to the type of energy contribution, as in the caption (sc or mc elec, side chain or main chain polar/electrostatic contributions, respectively; np, non-polar contributions). The following three crystal structures of  $G\alpha_{i1}$ –RGS complexes (with PDB codes) were superimposed:  $G\alpha_{i1}$ –RGS1 (2GTP),  $G\alpha_{i1}$ –RGS4 (1AGR), and  $G\alpha_{i1}$ –RGS16 (2IK8).  $G\alpha$  subunits are shown as ribbon diagrams, colored according to  $G\alpha$  domains: teal (GTPase domain) and olive (helical domain). A representative RGS domain (RGS16) is shown as a transparent orange molecular surface. (B)  $G\alpha_q$  residues that substantially contribute to interactions with RGS2 and RGS8, shown as spheres and colored as in (A). The crystal structures of  $G\alpha_q$ –RGS2 (4EKD) and  $G\alpha_q$ –RGS8 (5DO9) were superimposed and are shown as ribbon diagrams, colored according to  $G\alpha$  domains: blue (GTPase domain) and pink (helical domain). A representative RGS domain (RGS2) is shown as a transparent gray molecular surface. (C) A ribbon diagram of a representative complex ( $G\alpha_{i1}$ –RGS16) showing the location of the  $G\alpha$  GTPase and helical domains, and the three ‘switch regions’ that regulate interactions with  $G\alpha$  partners such as RGS domains. (D) 3D visualization as in A, rotated 90° about the  $y$ -axis. (E) 3D visualization as in B, rotated 90° about the  $y$ -axis. (F)  $G\alpha$  S&C residues, which contribute similarly to interactions with RGS domains across all  $G\alpha_i$  and  $G\alpha_q$  structures, are shown as red spheres.  $G_{i/q}$  specificity-determining residues, which contribute to specific interactions with RGS domains only in  $G\alpha_i$  or in  $G\alpha_q$  structures, are shown as purple spheres. All five structures shown in A and B were superimposed and are visualized as above.

contributing residues are found in the  $G\alpha$  GTPase domain, located exclusively in the three  $G\alpha$  switch regions; however, a third of the  $G\alpha$  residues that contribute significantly to interactions with RGS domains are located in the  $G\alpha$  helical domain (Figure 1A,B, cf. C). We next classified  $G\alpha$ -contributing residues into two major groups. The first group contains ‘Significant & Conserved (S&C) residues’, whose energy contributions are conserved across both  $G_i$  and  $G_q$  structures. Note that the conservation required in this group is of energy contributions, rather than sequence identity. However, we do observe that these residues not only contribute similarly to interactions with RGS domains, but that they are also conserved in sequence across the  $G_i$  and  $G_q$  subfamilies. The second group contains putative ‘ $G_{i/q}$  specificity-determining residues’, which contribute to RGS interactions only in the  $G\alpha_i$  or in the  $G\alpha_q$  structures. We hypothesized that the  $G_{i/q}$  specificity-determining residues, whose energy contributions differ between  $G\alpha_i$  and  $G\alpha_q$ , might underlie dissimilar interactions with RGS domains in general and with RGS2 in particular. Relevantly, we observed that  $G\alpha$  S&C residues are located solely in the GTPase domain, while  $G_{i/q}$  specificity-determining residues are mostly found in the  $G\alpha$  helical domain (Figure 1F). The later residues are located mostly in the  $\alpha A$  helix and in the  $\alpha B$ – $\alpha C$

loop in the helical domain (Supplementary Figure S2). Comparing these putative specificity-determining positions across the paralogs of  $G\alpha_{i1}$  and  $G\alpha_q$ , we saw that the subfamily-specific residues in these positions are conserved among the  $G_i$  homologs and among the  $G_q$  homologs that do interact, or do not interact with RGS2, respectively. Moreover, the residues in these positions diverge in the homologs of the visual G protein transducin ( $G\alpha_{t1-3}$ ), which are down-regulated by RGS9 and its homologs (Supplementary Figure S3). Therefore, the prevalence of  $G_{i/q}$  specificity-determining residues in the  $G\alpha$  helical domain suggested that these helical domain residues might determine  $G\alpha$  specificity toward RGS proteins and thus play a possible role in the unique specificity of RGS2 toward  $G\alpha_q$  and its homologs. We next compared these  $G\alpha_{i1}$  and  $G\alpha_q$  structures to identify which of these helical domain residues combine together into functional structural motifs that can discriminate between RGS domains.

## Replacing the $\alpha B$ – $\alpha C$ motif in the $G\alpha_{i1}$ helical domain with the corresponding $G\alpha_q$ residues increased RGS2 activity

Some of the putative  $G_{i/q}$  specificity-determining residues we identified are located in the  $\alpha B$ – $\alpha C$  loop of the  $G\alpha$  helical domain. This loop was previously shown to adopt different conformations in  $G\alpha_{i1}$  and  $G\alpha_q$  when bound to RGS8 and was thus suggested as being a potential selectivity determinant [17]. Therefore, we compared the  $\alpha B$ – $\alpha C$  loop (residues 112–120 in  $G\alpha_{i1}$  and residues 115–125 in  $G\alpha_q$ ) conformations and adjacent residues in the three  $G\alpha_{i1}$ –RGS and two  $G\alpha_q$ –RGS complexes. We observed that the region between  $G\alpha_i$  residues F108–F118 and  $G\alpha_q$  residues R114–A123, which includes the C-terminus of the  $\alpha B$  helix and most of the  $\alpha B$ – $\alpha C$  loop, adopts distinct conformations in each set of structures (Figure 2). We termed this structurally dissimilar region ‘the  $\alpha B$ – $\alpha C$  motif’. Interestingly, we note that this region has higher thermal B-factors in the three crystal structures of  $G\alpha_{i1}$ –RGS complexes than in the two  $G\alpha_q$ –RGS complexes (Supplementary Figure S4), suggesting that the  $\alpha B$ – $\alpha C$  motif also has a different dynamic behavior in the two  $G\alpha$  subfamilies. In contrast, the regions surrounding this segment were structurally aligned in all five structures and adopted very similar 3D conformations.

To test whether the  $\alpha B$ – $\alpha C$  motif plays a role in  $G\alpha$  specificity toward RGS2, we substituted this segment in  $G\alpha_{i1}$  with the corresponding residues from  $G\alpha_q$ . When the GAP activities of the RGS2 domain toward wild-type  $G\alpha_{i1}$  ( $G\alpha_{i1}$ -wt) and this chimera ( $G\alpha$ -i/q-1) were compared (Figure 3), we saw an increase in RGS2 activity, with the  $EC_{50}$  decreasing more than three-fold, from  $>10 \mu M$  ( $G\alpha_{i1}$ -wt) to  $3.2 \mu M$  ( $G\alpha$ -i/q-1). We note that the  $EC_{50}$  of RGS2 toward  $G\alpha_{i1}$ -wt is probably much higher than  $10 \mu M$ , given our inability to reach saturating concentrations of RGS2. However, the increased GAP activity of RGS2 toward the  $G\alpha$ -i/q-1 chimera was still much lower than the high GAP activity of RGS domains from the R4 family toward  $G\alpha_{i1}$ , which is in the tens of nM range [55]. Therefore, we next considered the individual  $G_{i/q}$  specificity-determining positions identified above and their potential roles in RGS2 interactions.

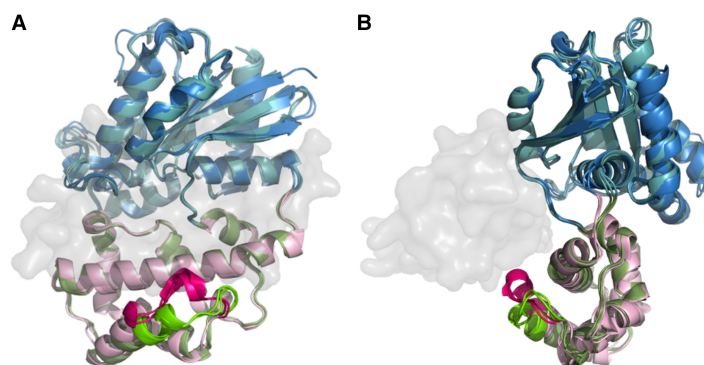


**Figure 2. The helical domains of  $G\alpha_i$  and  $G\alpha_q$  contain a structurally dissimilar region.**

(A) Superimposition of five crystal structures of  $G\alpha_{i1}$  and  $G\alpha_q$  complexed with RGS proteins, as in Figure 1F. The structurally dissimilar region, termed here the  $\alpha B$ – $\alpha C$  motif, consisting of residues F108–F118 in  $G\alpha_{i1}$  and R114–A123 in  $G\alpha_q$ , which includes the  $\alpha B$ – $\alpha C$  loop and some adjacent residues, is colored green ( $G\alpha_{i1}$ ) or magenta ( $G\alpha_q$ ). (B) Same as (A), rotated  $90^\circ$  about the  $y$ -axis ( $180^\circ$  about the  $y$ -axis, relative to Figure 1A,B).

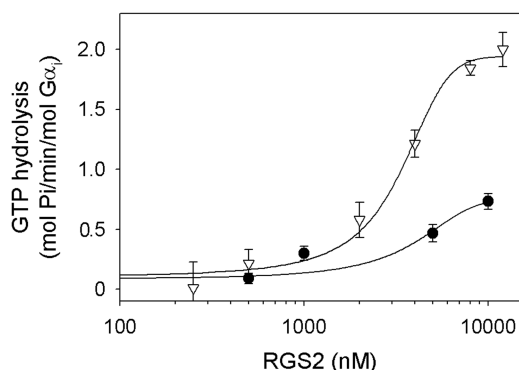


**Figure 3. Substitution of the  $\alpha$ B– $\alpha$ C motif in the  $G\alpha_{i1}$  helical domain with the corresponding residues from  $G\alpha_q$  increases RGS2 activity.**

Dose–response analysis of RGS2 activity toward wild-type  $G\alpha_{i1}$  (black circles) and the  $G\alpha$ -i/q-1 mutant (where the  $G\alpha_{i1}$   $\alpha$ B– $\alpha$ C motif, as defined in Figure 2, was replaced with the corresponding residues from  $G\alpha_q$ ; open triangles).  $EC_{50}$  values were calculated using three-parameter sigmoidal curves in SigmaPlot 10.0.  $EC_{50}$  of  $G\alpha_{i1}$ -wt >10 000 nM;  $EC_{50}$  of  $G\alpha$ -i/q-1 =  $3200 \pm 250$  nM. Data presented are means  $\pm$  s.e.m. of experiments performed in triplicate and are representative of three ( $G\alpha_{i1}$ -wt) and four ( $G\alpha$ -i/q-1) independent biological replicates each.

### Residues in the $G\alpha$ helical domain $\alpha$ A helix co-operate with the $\alpha$ B– $\alpha$ C motif to interact with RGS2

One of the substantial contributions identified in the  $\alpha$ B– $\alpha$ C motif was that of  $G\alpha_{i1}$ -E116, which forms an electrostatic and hydrogen bond network with a glutamate–lysine motif in the cognate RGS domain (E161 and K162 in RGS4; Figure 4A). This interaction is also conserved in the complexes of  $G\alpha_{i1}$  with RGS1 and RGS16 (Figure 4A). However, our calculations identified substantial contributions from three additional residues (A71, V72, and S75), all found in a different part of the  $G\alpha_{i1}$  helical domain, the  $\alpha$ A helix. These three residues

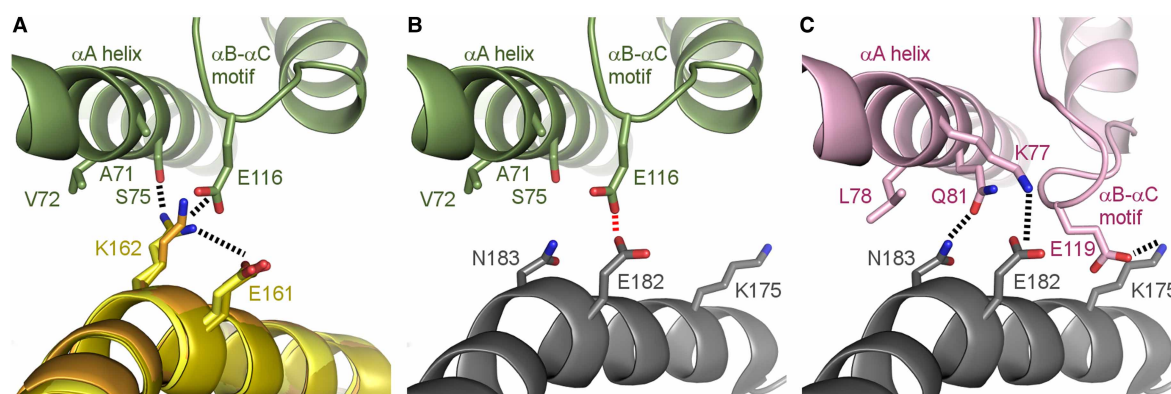


**Figure 4. The  $\alpha$ B– $\alpha$ C motif co-operates with  $G\alpha$   $\alpha$ A helix residues to interact with RGS domains.**

(A)  $G\alpha_{i1}$  helical domain residues that, together with the  $G\alpha_{i1}$   $\alpha$ B– $\alpha$ C motif, interact with a glutamate–lysine motif in RGS1, 4, and 16. Interacting residues are shown as sticks, with favorable electrostatic interactions/hydrogen bonds marked with dashed black lines. The  $G\alpha_{i1}$ -RGS1 (2GTP),  $G\alpha_{i1}$ -RGS4 (1AGR), and  $G\alpha_{i1}$ -RGS16 (2IK8) complexes are superimposed and shown as ribbon diagrams, colored olive ( $G\alpha_{i1}$  helical domain from 1AGR), dark-yellow (RGS1), yellow (RGS4), or orange (RGS16). Residues are numbered according to the  $G\alpha_{i1}$ -RGS4 structure. (B) Potential interactions of the  $G\alpha_{i1}$  helical domain residues shown in A with RGS2. RGS2 (from 4EKD, colored gray) was superimposed onto the RGS4- $G\alpha_{i1}$  complex and visualized as in A. Potential unfavorable interactions are marked with dashed red lines. (C) The corresponding  $G\alpha_q$ -RGS2 interactions in the  $G\alpha_q$ -RGS2 complex, visualized as in A, and colored pink ( $G\alpha_q$  helical domain) and gray (RGS2).

make a non-polar intermolecular contribution to interactions with the RGS residues mentioned above (Supplementary Figure S2) and to the RGS4-unique residue R166 (not shown). Importantly,  $G\alpha_{i1}$ -S75 also participates in the hydrogen bond network with the RGS glutamate–lysine motif (Figure 4A). These three  $G\alpha_{i1}$   $\alpha$ A helix residues also make intramolecular non-polar interactions with the  $\alpha$ B– $\alpha$ C loop (data not shown) and can thereby stabilize the loop in a particular conformation. As such, they also affect  $\alpha$ B– $\alpha$ C loop interactions with the RGS domain indirectly.

Further analysis by modeling the interactions of  $G\alpha_{i1}$  residues with RGS2 predicted that RGS2–E182 interacts unfavorably with  $G\alpha_{i1}$ –E116 (Figure 4B), and that the favorable interactions seen in Figure 4A would be lost in  $G\alpha_{i1}$  interactions with RGS2. In contrast, visualizing the comparable residues in  $G\alpha_q$  revealed a different interaction network across the interface with RGS2. Here, the  $G\alpha_q$   $\alpha$ B– $\alpha$ C motif adopted a distinct conformation from that seen in  $G\alpha_{i1}$ , with  $G\alpha_q$ –E119 forming an intermolecular salt bridge with RGS2–K175 (Figure 4C). This RGS2 residue is too far to interact favorably with  $G\alpha_{i1}$ –E116 (Figure 4B). The residues in the  $G\alpha_q$   $\alpha$ A helix also interact differently both across the interface and with the  $G\alpha_q$   $\alpha$ B– $\alpha$ C motif than do the corresponding  $G\alpha_{i1}$  residues (Figure 4C).  $G\alpha_q$ –K77 forms an intermolecular salt bridge with RGS2–E182.  $G\alpha_q$ –L78, which corresponds to  $G\alpha_{i1}$ –V72, makes a favorable non-polar intermolecular contribution to interactions with RGS2–N183 (not shown).  $G\alpha_q$ –Q81 forms a hydrogen bond with RGS2–N183 and also contributes an intramolecular non-polar interaction with the  $G\alpha_q$   $\alpha$ B– $\alpha$ C loop (not shown). We, therefore, predict that  $G\alpha_q$   $\alpha$ A helix residues K77, L78, and Q81 work together as a structural motif that co-operates with the  $\alpha$ B– $\alpha$ C motif in forming favorable interactions with RGS2. Accordingly, we added the corresponding  $G\alpha_{i1}$ -to- $G\alpha_q$  mutations (i.e. A71K, V72L, and S75Q) to the  $G\alpha$ -i/q-1 mutant to generate the  $G\alpha$ -i/q-2 mutant. Indeed, these additional changes increased RGS2 GAP activity toward this mutant, with the  $EC_{50}$  decreasing more than four-fold to 760 nM (Figure 5).

### $G\alpha_{i1}$ helical domain residues E65 and Q68 perturb interactions with RGS2

Two additional residues that can affect interactions with RGS2,  $G\alpha_{i1}$ –E65 and Q68, are located in the N-terminal portion of the  $G\alpha$   $\alpha$ A helix. These two residues form a structural motif that interact favorably with a lysine residue in high-activity RGS domains (K170 in RGS4, Figure 6A) via a salt bridge (with  $G\alpha_{i1}$ –E65) and a hydrogen bond (to  $G\alpha_{i1}$ –Q68). On the other hand, this position in RGS2 is occupied by a glutamate (E191), which is predicted to form unfavorable interactions with  $G\alpha_{i1}$ –E65 and might interact less favorably with  $G\alpha_{i1}$ –Q68 (Figure 6B). In  $G\alpha_q$ , the side chain of D71, which corresponds to  $G\alpha_{i1}$ –E65, is shorter and, therefore, likely to interact less unfavorably with RGS2–E191 (Figure 6C).  $G\alpha_q$ –G74, which corresponds to  $G\alpha_{i1}$ –Q68, does not interact at all with RGS residues (Figure 6C). Therefore, we predicted that  $G\alpha_{i1}$ –E65 and  $G\alpha_{i1}$ –Q68 perturb interactions with RGS2 more than do their  $G\alpha_q$  counterparts.

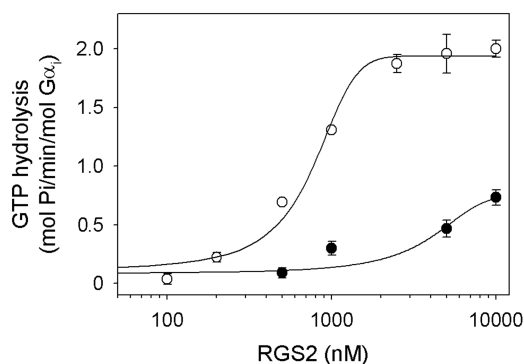


**Figure 5. Substitution of three additional  $\alpha$ A helix residues in the  $G\alpha_{i1}$  helical domain with the corresponding residues from  $G\alpha_q$  further increases RGS2 activity.**

Dose–response analysis of RGS2 activity toward the  $G\alpha$ -i/q-2 mutant ( $G\alpha$ -i/q-1 + A71K, V72L, S75Q; open circles).  $EC_{50}$  of  $G\alpha$ -i/q-2 =  $760 \pm 60$  nM. RGS2 activity toward wild-type  $G\alpha_{i1}$  (as in Figure 3) is shown for reference (black circles).  $EC_{50}$  values were calculated as in Figure 3. The data presented are means  $\pm$  s.e.m. of experiments performed in triplicate and are representative of three independent biological replicates each.

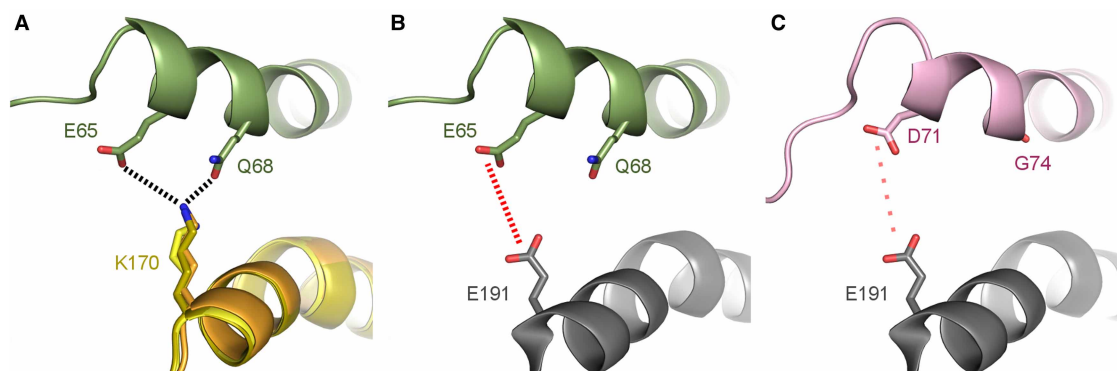


**Figure 6. Residues in the N-terminal portion of the  $G\alpha_{i1}$   $\alpha A$  helix may interact unfavorably with RGS2-E191.**

(A)  $G\alpha_{i1}$  helical domain residues that interact favorably with a lysine conserved in RGS1, 4, and 16. Interacting residues are shown as sticks, with favorable electrostatic interactions/hydrogen bonds marked with dashed black lines.  $G\alpha$  helical domains and RGS proteins are shown as in Figure 4. (B) Potential interactions of the  $G\alpha_{i1}$  helical domain residues shown in A with RGS2, as in Figure 4B. Potential unfavorable interactions are marked with dashed red lines. (C) The corresponding  $G\alpha_q$ -RGS2 interactions in the  $G\alpha_q$ -RGS2 complex, as in Figure 4C. Unfavorable interactions, which we predict are weaker than the unfavorable interactions modeled in Figure 6B, are marked with an orange dotted line.

To test these predictions, the appropriate mutants were generated. As hypothesized, replacing this motif ( $G\alpha_{i1}$ -E65 and Q68) with its  $G\alpha_q$  counterpart ( $G\alpha_q$ -D71 and G74) on the  $G\alpha$ -i/q-2 background (generating  $G\alpha$ -i/q-3) substantially decreased the  $EC_{50}$  to 330 nM (Figure 7). Further structural analysis identified an additional  $G\alpha_{i1}$  residue (K54) that can also affect the  $G\alpha_{i1}$ -RGS2 intermolecular interaction via intramolecular interactions with  $G\alpha_{i1}$ -E65. We hypothesized that, in  $G\alpha_q$ , the corresponding arginine residue might reduce the unfavorable interactions of D71 with RGS2-E191, when compared with  $G\alpha_{i1}$ -K54, because of the longer side chain and different geometry of the arginine residue (Supplementary Figure S5). Indeed, adding the K54R substitution to the  $G\alpha$ -i/q-3 mutant further decreased the  $EC_{50}$  of RGS2 toward the resulting  $G\alpha$ -i/q-4 mutant to 110 nM (Figure 7). In summary, substituting the  $\alpha B$ - $\alpha C$  motif and the additional  $G\alpha_{i1}$  helical domain residues identified here with their  $G\alpha_q$  counterparts increased the  $EC_{50}$  of RGS2 by more than two orders of magnitude (Figure 7).

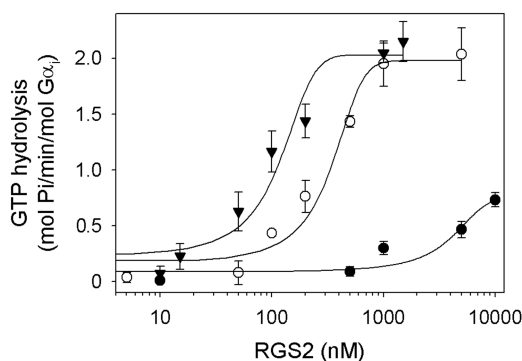


**Figure 7. Replacement of  $G\alpha_{i1}$  helical domain residues with their  $G\alpha_q$  counterparts further increases RGS2 activity.**

Dose-response analysis of RGS2 activity toward the  $G\alpha$ -i/q-3 mutant ( $G\alpha$ -i/q-2 + E65D + Q68G; open circles) and toward the  $G\alpha$ -i/q-4 mutant ( $G\alpha$ -i/q-3 + K54R; black triangles).  $EC_{50}$  of  $G\alpha$ -i/q-3 =  $330 \pm 50$  nM and  $G\alpha$ -i/q-4 =  $110 \pm 20$  nM. RGS2 activity toward wild-type  $G\alpha_{i1}$  (as in Figure 3) is shown for reference (black circles).  $EC_{50}$  values were calculated as in Figure 3. The data presented are means  $\pm$  s.e.m. of experiments performed in triplicate, representative of three ( $G\alpha$ -i/q-3) and four ( $G\alpha$ -i/q-4) independent biological replicates each.

## Discussion

Our results show that residues in the  $G\alpha$  helical domain play a major role in determining interaction specificity toward RGS2. While the  $G\alpha_q$ -RGS2 X-ray structure showed some RGS2 interaction with the  $G\alpha_q$  helical domain, mutation of selected individual  $G\alpha_q$  helical domain residues had only minor effects on the ability of RGS2 to interact with  $G\alpha_q$  [16]. Similarly, although  $G\alpha_q$  helical domain residues also interact with RGS8 in the  $G\alpha_q$ -RGS8 structure [17], mutagenesis experiments performed in this study, which had only minor effects on RGS interactions, also led to the conclusion that the helical domain is not a major selectivity determinant for such interaction. Rather, previous studies suggested that the unique sequence of RGS2 is the sole determinant of its dramatic selectivity for the  $G_i$  rather than the  $G_q$   $G\alpha$  subfamily [14–17,55], and that interactions with the  $G\alpha$  switch regions are critical mediators of this specificity [14–17,20]. However, we have shown here that  $G\alpha_{i1}$ -to- $G\alpha_q$  substitutions within the  $\alpha B$ - $\alpha C$  motif and the additional helical domain residues we identified are sufficient to produce a dramatic gain of function toward RGS2. The quantitative effect of changing these helical domain residues is similar to the gain-of-function effect of the RGS2 triple mutant (Supplementary Figure S6), which was characterized previously [15,55]. Since both the RGS2 triple mutant and the  $G\alpha$ -i/q-4 mutant increased GAP activity by more than two orders of magnitude (Supplementary Figures S6 and S7, respectively), and since the former was also shown to increase affinity by more than two orders of magnitude [15], it is likely that, in both cases, the increase in activity is due to a corresponding increase in affinity. Our results therefore suggest that the  $G\alpha$  helical domain plays a crucial role in determining specificity toward RGS proteins, and particularly in recognizing the unique RGS2 sequence/structure.

Structural moieties that determine specific interactions are often termed positive- and negative-design elements [63,64]. In the context of our work,  $G\alpha$  residues that contribute favorably to interactions with RGS2 act as positive-design elements, while  $G\alpha$  residues that perturb favorable interactions with RGS2 can be considered as negative-design elements. Accordingly, our results define the  $G\alpha_{i1}$   $\alpha B$ - $\alpha C$  motif as a positive-design element toward RGS1, 4, and 16, yet as a negative-design element toward RGS2. In addition, our computational analysis predicted that, in  $G\alpha_q$ , this motif is a positive-design element that interacts favorably with the unique residues in RGS2, a prediction that was validated by the increased activity of RGS2 toward the  $G\alpha$ -i/q-1 mutant. Furthermore, we suggest that three residues in the middle of the  $G\alpha_{i1}$   $\alpha A$  helix (A71, V72, and S75) form a structural motif that, together with the  $\alpha B$ - $\alpha C$  motif, functions as a positive-design element toward RGS1, 4, and 16. Conversely, the corresponding elements in  $G\alpha_q$  function together as positive-design elements toward RGS2. Indeed, substituting these  $G\alpha_{i1}$  residues with their  $G\alpha_q$  counterparts further increased RGS2 activity toward the  $G\alpha$ -i/q-2 mutant. Lastly, the two N-terminal  $G\alpha_{i1}$   $\alpha A$  helix residues E65 and Q68 function as a negative-design element toward RGS2, and substituting these residues with their  $G\alpha_q$  counterparts increased RGS2 activity even further.

The predicted combinations of  $G\alpha_{i1}$ -negative-design elements and  $G\alpha_q$ -positive-design elements that are missing in  $G\alpha_{i1}$  as explaining the differential recognition of RGS2 are supported by an additional experiment. When we mutated all of the  $G\alpha_{i1}$  residues mentioned above to alanines, the activity of RGS2 toward this mutant ( $G\alpha_{i1}$ -HD-Ala<sub>6</sub>) increased to a value similar to that measured with the  $G\alpha$ -i/q-1 mutant (Supplementary Figure S7). This suggests that negative design plays only a partial role in preventing RGS2 from interacting with  $G\alpha_i$  and that the positive-design elements in the  $G\alpha_q$  helical domain are required for achieving substantial RGS2 activity. We note that we did not investigate the potential role of water molecules or the dynamic properties of these proteins in mediating additional specificity-determining interactions, and further studies using complementary methods such as molecular dynamic simulations will probably expand our understanding of such determinants. Nevertheless, it is evident that the combination of the positive- and negative-design elements we identified in the  $G\alpha$  helical domain is sufficient to produce the extreme selectivity of the  $G_i$  versus the  $G_q$  subfamily in terms of RGS2 recognition.

In a broader context, previous work assigned specific and central roles for the  $G\alpha$  helical domain in nucleotide exchange [26] and in recognizing nucleotide exchange inhibitors [25]. Here, we identified a new and crucial role of the  $G\alpha$  helical domain, namely dictating specificity toward RGS2 in particular and RGS proteins in general. Our results provide a detailed mechanistic basis for further investigations of RGS-G protein interactions. In doing so, these findings raise the possibility of specifically manipulating RGS-G protein interactions *in vivo* so as to understand their ‘wiring’ into signaling networks, and for the development of drugs that target such interactions. The particular involvement of RGS2 in pathologies such as mental disorders, hypertension, cardiac hypertrophy, and cancer and the unique determinants of its specificity with the  $G_q$  subfamily further underscores how our findings can be used toward therapeutics that target these interactions.

## Abbreviations

FDPB, finite difference Poisson–Boltzmann; GAP, GTPase-activating protein; GPCRs, G protein-coupled receptors; RGS, regulators of G protein signaling; S&C, Significant & Conserved.

## Author Contribution

M.K. designed the research, conducted most of the experiments and structural analysis, analyzed results, and wrote the paper. S.G. conducted structural analysis and experiments, and analyzed results. I.S. conducted structural analysis and some experiments, and analyzed results. M.A-S. conducted experiments, supervised laboratory work, and analyzed results. M.K. designed and supervised the research, and wrote the paper. All the authors were involved in the writing of the paper and approved the final version.

## Funding

This work was supported by grants from the Israel Science Foundation [grant nos 1454/13, 1959/13, and 2155/15], the Israel Ministry of Science, Technology and Space, and the Italian Ministry of Foreign Affairs [3-10704].

## Acknowledgements

We thank Liza Barki-Harrington and Dan Cassel for helpful comments. The authors acknowledge the contribution of COST Action CM-1207 (GLISTEN) to this work.

## Competing Interests

The Authors declare that there are no competing interests associated with the manuscript.

## References

- 1 Sprang, S.R. (1997) G protein mechanisms: insights from structural analysis. *Annu. Rev. Biochem.* **66**, 639–678 <https://doi.org/10.1146/annurev.biochem.66.1.639>
- 2 Sprang, S.R., Chen, Z. and Du, X. (2007) Structural basis of effector regulation and signal termination in heterotrimeric  $G\alpha$  proteins. *Adv. Protein Chem.* **74**, 1–65 [https://doi.org/10.1016/S0065-3233\(07\)74001-9](https://doi.org/10.1016/S0065-3233(07)74001-9)
- 3 Oldham, W.M. and Hamm, H.E. (2008) Heterotrimeric G protein activation by G-protein-coupled receptors. *Nat. Rev. Mol. Cell Biol.* **9**, 60–71 <https://doi.org/10.1038/nrm2299>
- 4 Berman, D.M., Kozasa, T. and Gilman, A.G. (1996) The GTPase-activating protein RGS4 stabilizes the transition state for nucleotide hydrolysis. *J. Biol. Chem.* **271**, 27209–27212 <https://doi.org/10.1074/jbc.271.44.27209>
- 5 Hunt, T.W., Fields, T.A., Casey, P.J. and Peralta, E.G. (1996) RGS10 is a selective activator of  $G\alpha_i$  GTPase activity. *Nature* **383**, 175–177 <https://doi.org/10.1038/383175a0>
- 6 Koelle, M.R. and Horvitz, H.R. (1996) EGL-10 regulates G protein signaling in the *C. elegans* nervous system and shares a conserved domain with many mammalian proteins. *Cell* **84**, 115–125 [https://doi.org/10.1016/S0092-8674\(00\)80998-8](https://doi.org/10.1016/S0092-8674(00)80998-8)
- 7 Siderovski, D.P., Hessel, A., Chung, S., Mak, T.W. and Tyers, M. (1996) A new family of regulators of G-protein-coupled receptors? *Curr. Biol.* **6**, 211–212 [https://doi.org/10.1016/S0960-9822\(02\)00454-2](https://doi.org/10.1016/S0960-9822(02)00454-2)
- 8 Watson, N., Linder, M.E., Druey, K.M., Kehrl, J.H. and Blumer, K.J. (1996) RGS family members: GTPase-activating proteins for heterotrimeric G-protein  $\alpha$ -subunits. *Nature* **383**, 172–175 <https://doi.org/10.1038/383172a0>
- 9 Ross, E.M. and Wilkie, T.M. (2000) GTPase-activating proteins for heterotrimeric G proteins: regulators of G protein signaling (RGS) and RGS-like proteins. *Annu. Rev. Biochem.* **69**, 795–827 <https://doi.org/10.1146/annurev.biochem.69.1.795>
- 10 Kosloff, M., Travis, A.M., Bosch, D.E., Siderovski, D.P. and Arshavsky, V.Y. (2011) Integrating energy calculations with functional assays to decipher the specificity of G protein-RGS protein interactions. *Nat. Struct. Mol. Biol.* **18**, 846–853 <https://doi.org/10.1038/nsmb.2068>
- 11 Tesmer, J.J., Berman, D.M., Gilman, A.G. and Sprang, S.R. (1997) Structure of RGS4 bound to  $AlF_4^-$ -activated  $G\alpha_1$ : stabilization of the transition state for GTP hydrolysis. *Cell* **89**, 251–261 [https://doi.org/10.1016/S0092-8674\(00\)80204-4](https://doi.org/10.1016/S0092-8674(00)80204-4)
- 12 Slep, K.C., Kercher, M.A., He, W., Cowan, C.W., Wensel, T.G. and Sigler, P.B. (2001) Structural determinants for regulation of phosphodiesterase by a G protein at 2.0 Å. *Nature* **409**, 1071–1077 <https://doi.org/10.1038/35059138>
- 13 Slep, K.C., Kercher, M.A., Wieland, T., Chen, C.-K., Simon, M.I. and Sigler, P.B. (2008) Molecular architecture of  $G\alpha_o$  and the structural basis for RGS16-mediated deactivation. *Proc. Natl Acad. Sci. U.S.A.* **105**, 6243–6248 <https://doi.org/10.1073/pnas.0801569105>
- 14 Soundararajan, M., Willard, F.S., Kimple, A.J., Turnbull, A.P., Ball, L.J., Schoch, G.A. et al. (2008) Structural diversity in the RGS domain and its interaction with heterotrimeric G protein  $\alpha$ -subunits. *Proc. Natl Acad. Sci. U.S.A.* **105**, 6457–6462 <https://doi.org/10.1073/pnas.0801508105>
- 15 Kimple, A.J., Soundararajan, M., Hutsell, S.Q., Roos, A.K., Urban, D.J., Setola, V. et al. (2009) Structural determinants of G-protein  $\alpha$  subunit selectivity by regulator of G-protein signaling 2 (RGS2). *J. Biol. Chem.* **284**, 19402–19411 <https://doi.org/10.1074/jbc.M109.024711>
- 16 Nance, M.R., Kreuz, B., Tesmer, V.M., Sterne-Marr, R., Kozasa, T. and Tesmer, J.J. (2013) Structural and functional analysis of the regulator of G protein signaling 2- $G\alpha_q$  complex. *Structure* **21**, 438–448 <https://doi.org/10.1016/j.str.2012.12.016>
- 17 Taylor, V.G., Bommarito, P.A. and Tesmer, J.J. (2016) Structure of the regulator of G protein signaling 8 (RGS8)- $G\alpha_q$  complex: molecular basis for G- $\alpha$  selectivity. *J. Biol. Chem.* **291**, 5138–5145 <https://doi.org/10.1074/jbc.M115.712075>
- 18 Natochin, M. and Artemyev, N.O. (1998) Substitution of transducin Ser<sup>202</sup> by Asp abolishes G-protein/RGS interaction. *J. Biol. Chem.* **273**, 4300–4303 <https://doi.org/10.1074/jbc.273.8.4300>

- 19 Posner, B.A., Mukhopadhyay, S., Tesmer, J.J., Gilman, A.G. and Ross, E.M. (1999) Modulation of the affinity and selectivity of RGS protein interaction with  $G_{\alpha}$  subunits by a conserved asparagine/serine residue. *Biochemistry* **38**, 7773–7779 <https://doi.org/10.1021/bi9906367>
- 20 Mann, D., Teuber, C., Tennigkeit, S.A., Schröter, G., Gerwert, K. and Köting, C. (2016) Mechanism of the intrinsic arginine finger in heterotrimeric G proteins. *Proc. Natl Acad. Sci. U.S.A.* **113**, E8041–E8E50 <https://doi.org/10.1073/pnas.1612394113>
- 21 Neer, E.J. (1995) Heterotrimeric G proteins: organizers of transmembrane signals. *Cell* **80**, 249–257 [https://doi.org/10.1016/0092-8674\(95\)90407-7](https://doi.org/10.1016/0092-8674(95)90407-7)
- 22 Noel, J.P., Hamm, H.E. and Sigler, P.B. (1993) The 2.2 Å crystal structure of transducin- $\alpha$  complexed with GTP $\gamma$ S. *Nature* **366**, 654–663 <https://doi.org/10.1038/366654a0>
- 23 Markby, D.W., Onrust, R. and Bourne, H.R. (1993) Separate GTP binding and GTPase activating domains of a G alpha subunit. *Science* **262**, 1895–1901 <https://doi.org/10.1126/science.8266082>
- 24 Mixon, M.B., Lee, E., Coleman, D.E., Berghuis, A.M., Gilman, A.G. and Sprang, S.R. (1995) Tertiary and quaternary structural changes in  $G_{i\alpha 1}$  induced by GTP hydrolysis. *Science* **270**, 954–960 <https://doi.org/10.1126/science.270.5238.954>
- 25 Kimple, R.J., Kimple, M.E., Betts, L., Sondak, J. and Siderovski, D.P. (2002) Structural determinants for GoLoco-induced inhibition of nucleotide release by  $G_{\alpha}$  subunits. *Nature* **416**, 878–881 <https://doi.org/10.1038/416878a>
- 26 Rasmussen, S.G., DeVree, B.T., Zou, Y., Kruse, A.C., Chung, K.Y., Kobilka, T.S. et al. (2011) Crystal structure of the  $\beta 2$  adrenergic receptor–Gs protein complex. *Nature* **477**, 549–555 <https://doi.org/10.1038/nature10361>
- 27 Heximer, S.P., Watson, N., Linder, M.E., Blumer, K.J. and Hepler, J.R. (1997) RGS2/GOS8 is a selective inhibitor of Gq $\alpha$  function. *Proc. Natl Acad. Sci. U.S.A.* **94**, 14389–14393 <https://doi.org/10.1073/pnas.94.26.14389>
- 28 Heximer, S.P., Knutsen, R.H., Sun, X., Kaltenbronn, K.M., Rhee, M.-H., Peng, N. et al. (2003) Hypertension and prolonged vasoconstrictor signaling in RGS2-deficient mice. *J. Clin. Invest.* **111**, 445–452 <https://doi.org/10.1172/JCI15598>
- 29 Tang, K.M., Wang, G.R., Lu, P., Karas, R.H., Aronovitz, M., Heximer, S.P. et al. (2003) Regulator of G-protein signaling-2 mediates vascular smooth muscle relaxation and blood pressure. *Nat. Med.* **9**, 1506–1512 <https://doi.org/10.1038/nm958>
- 30 Takimoto, E., Koitabashi, N., Hsu, S., Ketner, E.A., Zhang, M., Nagayama, T. et al. (2009) Regulator of G protein signaling 2 mediates cardiac compensation to pressure overload and antihypertrophic effects of PDE5 inhibition in mice. *J. Clin. Invest.* **119**, 408–420 <https://doi.org/10.1172/JCI35620>
- 31 Tuomi, J.M., Chidiac, P. and Jones, D.L. (2010) Evidence for enhanced M3 muscarinic receptor function and sensitivity to atrial arrhythmia in the RGS2-deficient mouse. *Am. J. Physiol. Heart Circ. Physiol.* **298**, H554–H561 <https://doi.org/10.1152/ajpheart.00779.2009>
- 32 Zhang, W., Anger, T., Su, J., Hao, J., Xu, X., Zhu, M. et al. (2006) Selective loss of fine tuning of Gq/11 signaling by RGS2 protein exacerbates cardiomyocyte hypertrophy. *J. Biol. Chem.* **281**, 5811–5820 <https://doi.org/10.1074/jbc.M507871200>
- 33 Zhang, P., Su, J., King, M.E., Maldonado, A.E., Park, C. and Mende, U. (2011) Regulator of G protein signaling 2 is a functionally important negative regulator of angiotensin II-induced cardiac fibroblast responses. *Am. J. Physiol. Heart Circ. Physiol.* **301**, H147–H156 <https://doi.org/10.1152/ajpheart.00026.2011>
- 34 Nlend, M.-C., Bookman, R.J., Conner, G.E. and Salathe, M. (2002) Regulator of G-protein signaling protein 2 modulates purinergic calcium and ciliary beat frequency responses in airway epithelia. *Am. J. Respir. Cell Mol. Biol.* **17**, 436–445 <https://doi.org/10.1165/rcmb.2002-00120C>
- 35 Xie, Y., Jiang, H., Nguyen, H., Jia, S., Berro, A., Panettieri, Jr, R.A. et al. (2012) Regulator of G protein signaling 2 is a key modulator of airway hyperresponsiveness. *J. Allergy Clin. Immunol.* **130**, 968–976.e3 <https://doi.org/10.1016/j.jaci.2012.05.004>
- 36 Oliveira-Dos-Santos, A.J., Matsumoto, G., Snow, B.E., Bai, D., Houston, F.P., Whishaw, I.Q. et al. (2000) Regulation of T cell activation, anxiety, and male aggression by RGS2. *Proc. Natl Acad. Sci. U.S.A.* **97**, 12272–12277 <https://doi.org/10.1073/pnas.220414397>
- 37 Ingi, T., Krumins, A.M., Chidiac, P., Brothers, G.M., Chung, S., Snow, B.E. et al. (1998) Dynamic regulation of RGS2 suggests a novel mechanism in G-protein signaling and neuronal plasticity. *J. Neurosci.* **18**, 7178–7188 <https://doi.org/10.1523/JNEUROSCI.18-18-07178.1998>
- 38 Han, J., Mark, M.D., Li, X., Xie, M., Waka, S., Rettig, J. et al. (2006) RGS2 determines short-term synaptic plasticity in hippocampal neurons by regulating  $G_{i\alpha}$ -mediated inhibition of presynaptic  $Ca^{2+}$  channels. *Neuron* **51**, 575–586 <https://doi.org/10.1016/j.neuron.2006.07.012>
- 39 Labouèbe, G., Lomazzi, M., Cruz, H.G., Creton, C., Luján, R., Li, M. et al. (2007) RGS2 modulates coupling between GABAB receptors and GIRK channels in dopamine neurons of the ventral tegmental area. *Nat. Neurosci.* **10**, 1559–1568 <https://doi.org/10.1038/nn2006>
- 40 Yalcin, B., Willis-Owen, S.A., Fullerton, J., Meesaq, A., Deacon, R.M., Rawlins, J.N. et al. (2004) Genetic dissection of a behavioral quantitative trait locus shows that RGS2 modulates anxiety in mice. *Nat. Genet.* **36**, 1197–1202 <https://doi.org/10.1038/ng1450>
- 41 Amstadter, A.B., Koenen, K.C., Ruggiero, K.J., Acierno, R., Galea, S., Kilpatrick, D.G. et al. (2009) Variant in RGS2 moderates posttraumatic stress symptoms following potentially traumatic event exposure. *J. Anxiety Disord.* **23**, 369–373 <https://doi.org/10.1016/j.janxdis.2008.12.005>
- 42 Lifschytz, T., Broner, E.C., Zozulinsky, P., Slonimsky, A., Eitan, R., Greenbaum, L. et al. (2012) Relationship between RGS2 gene expression level and anxiety and depression-like behaviour in a mutant mouse model: serotonergic involvement. *Int. J. Neuropsychopharmacol.* **15**, 1307–1318 <https://doi.org/10.1017/S1461145711001453>
- 43 Calo, L.A., Pagnin, E., Davis, P.A., Sartori, M., Ceolotto, G., Pessina, A.C. et al. (2004) Increased expression of regulator of G protein signaling-2 (RGS-2) in Bartter's/Gitelman's syndrome. A role in the control of vascular tone and implication for hypertension. *J. Clin. Endocrinol. Metabolism* **89**, 4153–4157
- 44 Gu, S., Tirgari, S. and Heximer, S.P. (2008) The RGS2 gene product from a candidate hypertension allele shows decreased plasma membrane association and inhibition of Gq. *Mol. Pharmacol.* **73**, 1037–1043 <https://doi.org/10.1124/mol.107.044214>
- 45 Semplicini, A., Strapazzon, G., Papparella, I., Sartori, M., Realdi, A., Macchini, L. et al. (2010) RGS2 expression and aldosterone: renin ratio modulate response to drug therapy in hypertensive patients. *J. Hypertens.* **28**, 1104–1108 <https://doi.org/10.1097/HJH.0b013e328339930f>
- 46 Osei-Owusu, P., Sabharwal, R., Kaltenbronn, K.M., Rhee, M.-H., Chappelle, M.W., Dietrich, H.H. et al. (2012) Regulator of G protein signaling 2 deficiency causes endothelial dysfunction and impaired endothelium-derived hyperpolarizing factor-mediated relaxation by dysregulating  $G_{i\alpha}$  signaling. *J. Biol. Chem.* **287**, 12541–12549 <https://doi.org/10.1074/jbc.M111.332130>
- 47 Nunn, C., Zou, M.-X., Sobiesiak, A.J., Roy, A.A., Kirshenbaum, L.A. and Chidiac, P. (2010) RGS2 inhibits  $\beta$ -adrenergic receptor-induced cardiomyocyte hypertrophy. *Cell. Signal.* **22**, 1231–1239 <https://doi.org/10.1016/j.cellsig.2010.03.015>
- 48 Kim, D.H., Lim, J.J., Lee, J.J., Kim, D.G., Lee, H.J., Min, W. et al. (2012) RGS2-mediated intracellular  $Ca^{2+}$  level plays a key role in the intracellular replication of *Brucella abortus* within phagocytes. *J. Infect. Dis.* **205**, 445–452 <https://doi.org/10.1093/infdis/jir765>

- 49 Cao, X., Qin, J., Xie, Y., Khan, O., Dowd, F., Scofield, M. et al. (2006) Regulator of G-protein signaling 2 (RGS2) inhibits androgen-independent activation of androgen receptor in prostate cancer cells. *Oncogene* **25**, 3719–3734 <https://doi.org/10.1038/sj.onc.1209408>
- 50 Hurst, J.H. and Hooks, S.B. (2009) Regulator of G-protein signaling (RGS) proteins in cancer biology. *Biochem. Pharmacol.* **78**, 1289–1297 <https://doi.org/10.1016/j.bcp.2009.06.028>
- 51 Jiang, Z., Wang, Z., Xu, Y., Wang, B., Huang, W. and Cai, S. (2010) Analysis of RGS2 expression and prognostic significance in stage II and III colorectal cancer. *Biosci. Rep.* **30**, 383–390 <https://doi.org/10.1042/BSR20090129>
- 52 Boelte, K.C., Gordy, L.E., Joyce, S., Thompson, M.A., Yang, L. and Lin, P.C. (2011) RGS2 mediates pro-angiogenic function of myeloid derived suppressor cells in the tumor microenvironment via upregulation of MCP-1. *PLoS ONE* **6**, e18534 <https://doi.org/10.1371/journal.pone.0018534>
- 53 Wolff, D.W., Xie, Y., Deng, C., Gatalica, Z., Yang, M., Wang, B. et al. (2012) Epigenetic repression of regulator of G-protein signaling 2 promotes androgen-independent prostate cancer cell growth. *Int. J. Cancer* **130**, 1521–1531 <https://doi.org/10.1002/ijc.26138>
- 54 Lyu, J.H., Park, D.-W., Huang, B., Kang, S.H., Lee, S.J., Lee, C. et al. (2015) RGS2 suppresses breast cancer cell growth via a MCP1P1-dependent pathway. *J. Cell. Biochem.* **116**, 260–267 <https://doi.org/10.1002/jcb.24964>
- 55 Heximer, S.P., Srinivasa, S.P., Bernstein, L.S., Bernard, J.L., Linder, M.E., Hepler, J.R. et al. (1999) G protein selectivity is a determinant of RGS2 function. *J. Biol. Chem.* **274**, 34253–34259 <https://doi.org/10.1074/jbc.274.48.34253>
- 56 Petrey, D., Xiang, Z., Tang, C.L., Xie, L., Gimpelev, M., Mitros, T. et al. (2003) Using multiple structure alignments, fast model building, and energetic analysis in fold recognition and homology modeling. *Proteins Struct., Funct. Genet.* **53**(Suppl 6), 430–435 <https://doi.org/10.1002/prot.10550>
- 57 Xiang, Z. and Honig, B. (2001) Extending the accuracy limits of prediction for side-chain conformations. *J. Mol. Biol.* **311**, 421–430 <https://doi.org/10.1006/jmbi.2001.4865>
- 58 Zur, Y., Rosenfeld, L., Bakhman, A., Ilic, S., Hayun, H., Shahar, A. et al. (2017) Engineering a monomeric variant of macrophage colony-stimulating factor (M-CSF) that antagonizes the c-FMS receptor. *Biochem. J.* **474**, 2601–2617 <https://doi.org/10.1042/BCJ20170276>
- 59 Rabinovich, E., Heyne, M., Bakhman, A., Kosloff, M., Shifman, J.M. and Papo, N. (2017) Identifying residues that determine SCF molecular-level interactions through a combination of experimental and *in silico* analyses. *J. Mol. Biol.* **429**, 97–114 <https://doi.org/10.1016/j.jmb.2016.11.018>
- 60 Sheinerman, F.B., Al-Lazikani, B. and Honig, B. (2003) Sequence, structure and energetic determinants of phosphopeptide selectivity of SH2 domains. *J. Mol. Biol.* **334**, 823–841 <https://doi.org/10.1016/j.jmb.2003.09.075>
- 61 Nicholls, A., Sharp, K.A. and Honig, B. (1991) Protein folding and association: insights from the interfacial and thermodynamic properties of hydrocarbons. *Proteins* **11**, 281–296 <https://doi.org/10.1002/prot.340110407>
- 62 Mukhopadhyay, S. and Ross, E.M. (1999) Rapid GTP binding and hydrolysis by Gq promoted by receptor and GTPase-activating proteins. *Proc. Natl Acad. Sci. U.S.A.* **96**, 9539–9544 <https://doi.org/10.1073/pnas.96.17.9539>
- 63 Havranek, J.J. and Harbury, P.B. (2003) Automated design of specificity in molecular recognition. *Nat. Struct. Biol.* **10**, 45–52 <https://doi.org/10.1038/nsb877>
- 64 Schreiber, G. and Keating, A.E. (2011) Protein binding specificity versus promiscuity. *Curr. Opin. Struct. Biol.* **21**, 50–61 <https://doi.org/10.1016/j.sbi.2010.10.002>

## Supplementary Information

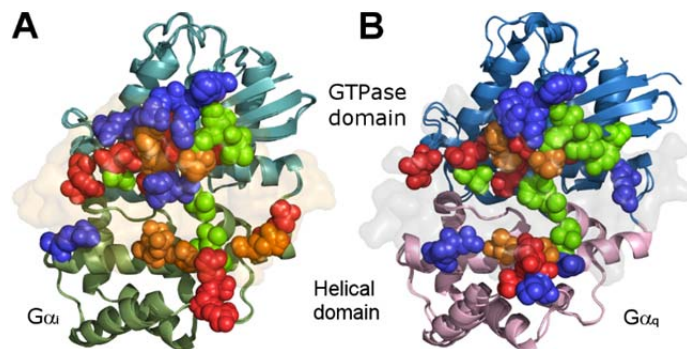


**Figure S1: The physicochemical classification of  $G\alpha_i$  and  $G\alpha_q$  residues that contribute significantly to interactions with RGS domains.** **A.**  $G\alpha_i$  residues that contribute significantly to the interaction with RGS subunits (as in Fig. 1D), shown as spheres and colored as follows: basic residues, blue; acidic residues, red; polar residues, orange; all other residues, green. The three representative structures of  $G\alpha_i$  subunits and the RGS domain are visualized as in Fig. 1D. **B.**  $G\alpha_q$  residues that contribute significantly to the interaction with RGS subunits (as in Fig. 1E), shown as spheres and colored as in A. The two representative structures of the  $G\alpha_q$  subunits and the RGS domain are visualized as in Fig. 1E.

Residue num ( $G\alpha_{i1}$ )	60	70	80	90	100	110	120
	αA			αB		αB-αC loop	
$G_{i1}$ (2IK8)	54	KIIHEAGYSEEECKQYKAVVYSNTIISIIAIIIRAMG	80	90	100	110	120
$G_{i1}$ (1AGR)	54	KIIHEAGYSEEECKQYKAVVYSNTIQSIIAIIIRAMG	80	90	100	110	120
$G_{i1}$ (2GTP)	54	KIIHEAGYSEEECKQYKAVVYSNTIISIIAIIIRAMG	80	90	100	110	120
$G_q$ (4EKD)	60	RIIHGSGYSDEDKRGFTKLVYQNIFFAMQAMIRAMDTLKI	80	90	100	110	120
$G_q$ (5DO9)	60	RIIHGSGYSDEDKRGFTKLVYQNIFFAMQAMIRAMDTLKI	80	90	100	110	120

**Figure S2: Significantly contributing residues in the  $G\alpha_i$  and  $G\alpha_q$  helical domains.** A residue-level sequence map summarizing our structure-based energy calculations of the representative  $G\alpha_i$  and  $G\alpha_q$  complexes with RGS proteins (as in Fig. 1). Colored boxes mark  $G\alpha$  residues that contribute substantially to interactions with RGS proteins in each structure (with PDB IDs on the left) – magenta (side-chain polar/electrostatic and non-polar contributions), red (side-chain polar/electrostatic contribution only), cyan (main-chain polar/electrostatic and nonpolar contributions), or green (non-polar contribution only). Relevant  $G\alpha$  secondary structure elements are marked above the alignment.



**Fig S3: Comparison of helical domain residues that contribute to interactions with RGS domains in  $G\alpha_{i1}$ ,  $G\alpha_q$ , and their related paralogs.** The related human homologs of  $G\alpha_{i1}$  and  $G\alpha_q$  (UNIPROT sequences:  $G\alpha_{i1}$ , P63096;  $G\alpha_{i2}$ , P04899;  $G\alpha_{i3}$ , P08754;  $G\alpha_o$ , P09471;  $G\alpha_{i1}$ , P11488;  $G\alpha_{i2}$ , P19087;  $G\alpha_{i3}$ , A8MTJ3;  $G\alpha_q$ , P50148;  $G\alpha_{i1}$ , P29992;  $G\alpha_{i4}$ , O95837) were aligned using the MAFFT server (<https://mafft.cbrc.jp/alignment/server/>) and visualized using the BoxShade server ([https://embnet.vital-it.ch/software/BOX\\_form.html](https://embnet.vital-it.ch/software/BOX_form.html)). Identical residues in the majority of sequences are shaded black, and conserved residues are shaded gray. Residues that make direct contributions to interactions with RGS proteins (as in Fig. S2) are marked above the alignment as follows: non-polar contributions (green plus signs), side chain contributions (red cross), side chain contributions and non-polar contributions (magenta double crosses).

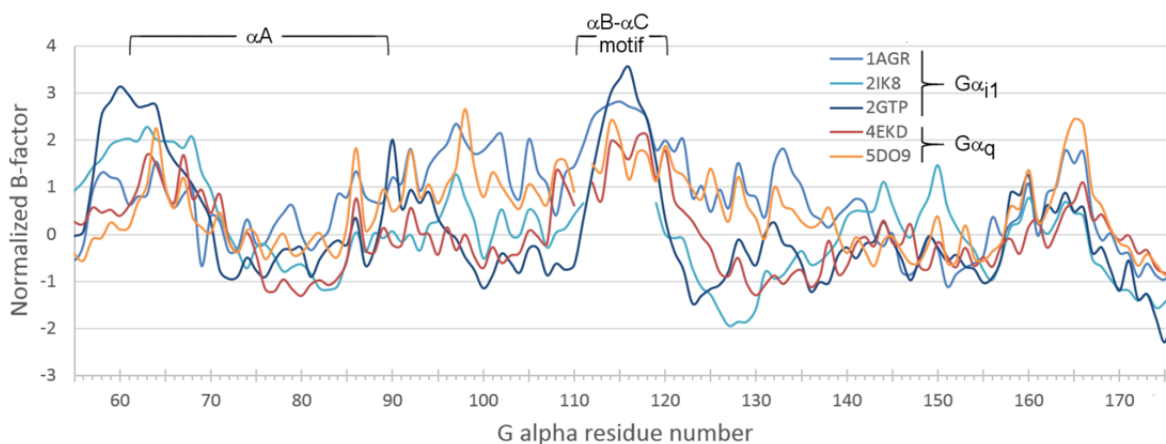


**Fig S4: Normalized thermal B-factors for the helical domain of  $G\alpha_{i1}$  and  $G\alpha_q$  in complex with RGS domains.** B-factors were taken from the same five crystal structures analyzed in Figs. 1, S1, and S2 (with PDB codes):  $G\alpha_{i1}$ -RGS1 (2GTP),  $G\alpha_{i1}$ -RGS4 (1AGR),  $G\alpha_{i1}$ -RGS16 (2IK8),  $G\alpha_q$ -RGS2 (4EKD), and  $G\alpha_q$ -RGS8 (5DO9).

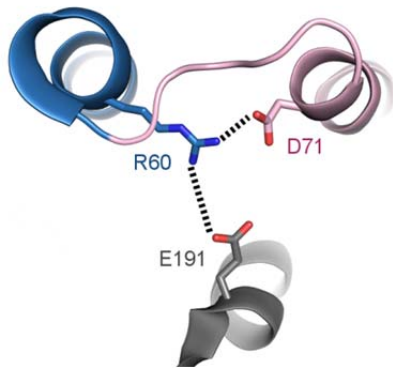


**Figure S5:  $G\alpha_q$ -R60 can affect the unfavorable interaction of  $G\alpha_q$ -D71 with RGS2-E191.**  $G\alpha_q$ -R60 forms an electrostatic inter- and intra-molecular network with  $G\alpha_q$ -D71 and RGS2-E191, visualized as in Fig. 4C, with the  $G\alpha_q$  GTPase domain colored blue.

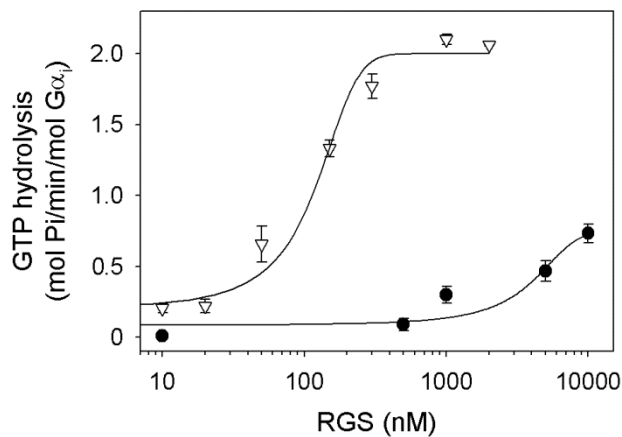


**Figure S6: The RGS2-SDK triple mutant increased GAP activity.** Dose-response analysis of the RGS2-SDK (C106S, N184D, E191K) triple mutant (white triangles);  $EC_{50} = 120 \pm 20$  nM. RGS2 activity towards wild type  $G\alpha_{i1}$  (black circles), as in Fig. 3, is shown for reference.  $EC_{50}$  values were calculated as in Fig. 3. Data presented are means  $\pm$  s.e.m. of experiments performed in triplicate, and are representative of three independent biological replicates each.

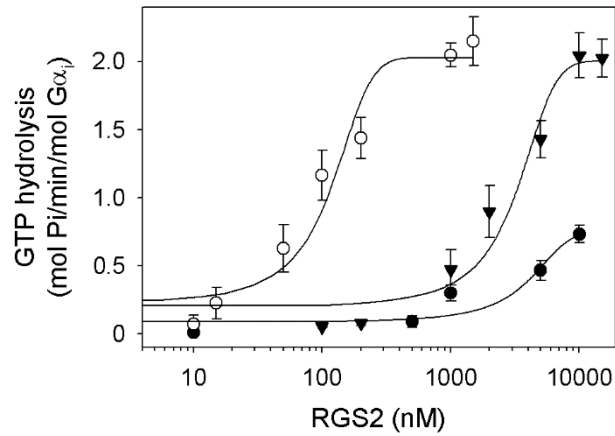


**Figure S7: Substituting  $G\alpha_{i1}$  helical domain residues that interact with RGS domains with alanines increase RGS2 activity.** Dose-response analysis of RGS2 activity towards the  $G\alpha_{i1}$ -HD-Ala<sub>6</sub> mutant, in which all six  $G\alpha_{i1}$  residues that contribute to RGS interactions, as in Fig. 1A, are replaced with alanines (black triangles).  $EC_{50}$  of  $G\alpha_{i1}$ -HD-Ala<sub>6</sub> =  $3100 \pm 550$  nM. RGS2 activity towards wild type  $G\alpha_{i1}$  (black circles) and  $G\alpha$ -i/q-4 (open circles), as in Fig. 7, is shown for reference.  $EC_{50}$  values were calculated as in Fig. 3. Data presented are means  $\pm$  s.e.m. of experiments performed in triplicate, and are representative of three ( $G\alpha_{i1}$ -HD-Ala<sub>6</sub>) independent biological replicates each.